Spatial filtering of light by chirped photonic crystals

Kestutis Staliunas[1] and Victor J. Sánchez-Morcillo[2]
[1]*ICREA, Departament de Fisica i Enginyeria Nuclear, Universitat Politècnica de Catalunya, Colom 11, E-08222 Terrassa, Barcelona, Spain*
[2]*Instituto de Investigación para la Gestión Integrada de Zonas Costeras, Universidad Politécnica de Valencia, Ctra. Natzaret-Oliva S/N, 46730 Grao de Gandía, Spain*
(Received 30 September 2008; published 5 May 2009)

We propose an efficient method for spatial filtering of light beams by propagating them through two-dimensional (also three dimensional) chirped photonic crystals, i.e., through the photonic structures with fixed transverse lattice period and with the longitudinal lattice period varying along the direction of the beam propagation. We prove the proposed idea by numerically solving the paraxial propagation equation in refraction-index–modulated media and we evaluate the efficiency of the process by harmonic-expansion analysis. The technique can be also applied for filtering (for cleaning) of the packages of atomic waves (Bose condensates), also to improve the directionality of acoustic and mechanical waves.

DOI: 10.1103/PhysRevA.79.053807 PACS number(s): 42.25.Fx, 42.55.Tv, 42.79.−e

I. INTRODUCTION

Many applications in optics require the use of beams of a good spatial quality characterized by a smooth envelope and, respectively, a narrow spatial spectrum. The "clean" beams diverge less in propagation, they can be focused more tightly, and they are more robust against nonlinear filamentation than the "dirty" ones. In laser science, the spatial quality of the beam is usually characterized by the beam parameter product (BPP), which is the product of a laser beam divergence angle (the half-angle) and the radius of the beam at its narrowest point (the beam waist) [1]. The BPP quantifies the quality of a laser beam and specifies how tight it can be focused. A Gaussian beam has the lowest possible BPP, λ/π, where $\lambda=2\pi c/\omega$ is the wavelength of the light [1]. The ratio of the BPP of a beam to that of a Gaussian beam at the same wavelength is denoted M^2 ("M squared"). This parameter is a wavelength-independent measure of beam quality and increases as the beam quality decreases. The single-transverse-mode lasers emit "clean" Gaussian beams" ($M^2=1$); however the beams emitted by many optical devices (multi-transverse-mode lasers, optical parametric oscillators) are often not smooth and of poor spatial quality ($M^2>1$). The propagation of light beams through various optical components, such as laser amplifiers, nonlinear materials, scattering media, or thermolensing media, also usually reduces the quality of the beam.

In order to improve the spatial quality of the beams, they are to be "cleaned" or spatially filtered. Usually in practice the cleaning of beams is achieved by the use of a telescope, consisting of two focusing lenses in a confocal arrangement and a pinhole in the focus point [2]. The pinhole lets to pass the low spatial Fourier components and removes the high ones (related to the beam inhomogeneities); therefore the beam after the spatial filter is of improved spatial quality. This system, although widely used, has several disadvantages, as a relatively large size (several centimeters for a visible light), high sensitivity to alignment (since the focused beam must past exactly through the middle of the pinhole) or the absence of efficient focusing lenses in infrared and in ultraviolet frequencies.

In the present paper, another alternative method for the spatial filtering is proposed, free from the above disadvantages. In the proposed method the beam propagates through a specially designed photonic crystal (PC). The filtering is based on the fact that the energy flow (the group velocity) of each spatial frequency component is determined by the gradient of the frequency in $\vec{k}$ space $\vec{v}=d\omega/d\vec{k}$ [$\vec{k}=(k_\perp,k_\parallel)$ is the propagation wave vector], or equivalently, is directed perpendicularly of the spatial dispersion curves $k_\parallel=k_\parallel(k_\perp)$, which are the isofrequency lines in the $\vec{k}$ space: $\omega(\vec{k})=$const. Figure 1 shows the spatial dispersion curves of the Bloch waves in periodically modulated material. In the proposed filtering method, the undesired spatial spectra components (those lying on the strongly tilted segments of the spatial dispersion curve) are strongly deflected; whereas the "clean" part of the beam, consisting of the central part of the spatial spectrum (those lying on the segment of the spatial dispersion curves which are nearly parallel to the corre-

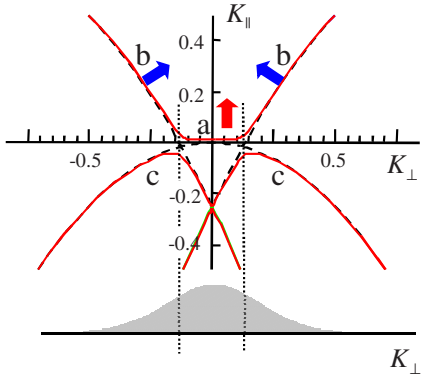

FIG. 1. (Color online) The dispersion curves of the Bloch modes in (unchirped) PC (solid lines) and of the harmonic components (dashed lines). At the bottom, the spatial spectrum of the beam consisting of the central (regular) part, and the wings (the part to be filtered) is illustrated. Parameters $Q_\parallel=0.75$, $f=0.04$. The sector a indicates the plateau (relevant for the self-collimation), the sectors b indicate the strongly tilted segments (relevant for the filtering), and the sectors c indicate the "useless" (nonfiltering) Bloch modes.

sponding plane-wave components,) propagates through (and behind) the crystal without sensible deflection.

We describe below the method of spatial filtering in PCs and demonstrate its feasibility by the numerical integration of the paraxial model of the wave propagation accounting explicitly for the spatial modulation of the refractive index. We also evaluate the efficiency of the process and the parameter range of efficient filtering by an analytical-numerical study in the framework of a truncated expansion into field harmonics.

The proposed method is extendable to the other types of waves in the nature. As the effect of spatial filtering is indirectly related with the effect of self-collimation or subdiffraction [3–5] then the filtering could be expected in all systems where the subdiffraction is possible; such systems are, e.g., the Bose-Einstein condensates (BECs) in spatiotemporally periodic potentials, where matter wave packets can behave subdiffractively [6,7]. (Here the propagation along the longitudinal direction in optics corresponds to the evolution in time for BECs.) The spatial filtering can be also obtained in the periodic acoustic systems (so-called sonic crystals), where the mechanical (sound) waves can also propagate without diffraction [8]. In this way the predicted phenomenon of spatial filtering is common for the waves of different nature propagating in periodically modulated materials and thus bears a universal character. The above-mentioned indirect relation between the spatial filtering method proposed here and the above mentioned self-collimation effect is basically the following. The strongly tilted segments in the spatial dispersion curve, which are responsible for the filtering effect, appear at approximately the same frequencies where a bounded region of the dispersion curve becomes flat (see Fig. 1). In fact the appearance of the central plateau is (always) related with formation of the tilted segments. Therefore the filtering of narrow or of noisy beams on one hand and the self-collimation on another hand are expected to occur for similar frequencies and are the effects of the similar physical origin.

II. MODEL

The propagation of light in a material with harmonic refraction index modulation is described, in paraxial approximation, by the Shrödinger-type equation

$$\frac{\partial A}{\partial Z} = i\left[\frac{\partial^2}{\partial X^2} + 4f\cos(Q_\parallel Z)\cos(X)\right]A, \tag{1}$$

where $A(X,Z)$ is the slowly varying envelope of the monochromatic electromagnetic field. The normalizations are adapted from [5], where $X=xq_\perp$ is the normalized transverse coordinate ($q_\perp$ is the transverse component of the wave vector of index modulation); $Z=zq_\perp^2/2k_0$ is the normalized longitudinal coordinate ($k_0=2\pi/\lambda$ is the wave number of the incident monochromatic light); $Q_\parallel(Z)=2q_\parallel(z)k_0/q_\perp^2$ is the normalized longitudinal component of the wave vector of the index modulation (longitudinal PC lattice constant), which—in general—is considered to depend on Z. In the latter case, the (nearly) periodic structure of the PC contains a longitudinal chirp. In subsequent numerical and analytical study we consider the linear chirp $dQ_\parallel/dZ=$const; however the various chirp functions are in general possible (and, perhaps, can be more efficient than the linear one). The normalized modulation parameter $f=\Delta n k_0^2/2q_\perp^2$ is related to the refraction index modulation in original variables via $n(x,z)=n_0[1+\Delta n\cos(q_\perp x)\cos(q_\parallel z)]$. The modulation is considered harmonic throughout the paper without loss of generality, as the effects of the spatial propagation in modulated materials in first order depends on the symmetry of the lattice and less on the concrete shape of the modulation. The relation of normalized parameters in Eq. (1) with the physical parameters in other spatially modulated systems can be found, e.g., for BECs in [6], and for acoustic waves in [8].

III. HARMONIC EXPANSION

For the analytical study, we assume that the chirp is weak $|dQ_\parallel/dZ|\ll 1$ (or equivalently $|dq_\parallel/dz|\ll 4k_0^2/q_\perp^4$ in the original optical variables) and expand the field in spatial harmonics of the PC structure (analogously to the unchirped case, e.g., in [5]),

$$A(X,Z) = e^{iK_\perp X}\sum_{l,m} A_{l,m}(Z)e^{i\vec{Q}_{l,m}\vec{R}}, \tag{2}$$

where $\vec{Q}_{l,m}=(l,mQ_\parallel)$, l, $m=..-2,-1,0,1,2...$ is the set of the reciprocal-lattice vectors in the normalized wave-vector space $\vec{K}=(K_\perp,K_\parallel)$; $\vec{R}=(X,Z)$ is the normalized physical space. The expansion (2) converts Eq. (1) into a coupled system for the evolution of the amplitudes of the harmonics,

$$\frac{dA_{l,m}(Z)}{dZ} = -i[(l+K_\perp)^2 + mQ_\parallel(Z)]A_{l,m}(Z) + if\sum_{|r-l|=1,|p-m|=1} A_{r,p}(Z), \tag{3}$$

where the Z dependence of $Q_\parallel(Z)$ mimics the longitudinal chirp. In the absence of the chirp, one obtains the steady propagation of the Bloch waves $A_{l,m}(Z)\propto e^{iK_\parallel Z}$, and the solvability of Eq. (3) results in the transverse dispersion relation of the Bloch waves of the PC, $K_\parallel(K_\perp)$.

For the study of self-collimation, as shown in [5,6], the expansion (2) is to be truncated to the three most relevant harmonics [respectively, to the five harmonics in the three-dimensional (3D) case [7]]. We adopt this approximation also here by considering the central harmonics $\vec{Q}_{0,0}=(0,0)$ and the first sideband components $\vec{Q}_{-1,\pm 1}=(-1,\pm Q_\parallel)$, corresponding to plane-waves (harmonics) with the propagation wave vectors $\mathbf{K}=(K_\perp,K_\parallel)$ and $\mathbf{K}=(K_\perp\pm 1,K_\parallel+Q_\parallel)$, respectively, as their dispersion curves cross at the point $\mathbf{K}=(0,0)$ for $Q_\parallel=1$ (the triple-cross point).

The dispersion curves of the harmonic components and of the Bloch modes are shown in Fig. 1 by the dashed and the solid lines, respectively. The Bloch mode most relevant to our analysis displays, at particular frequencies, a plateau in the central part around $K_\perp\approx 0$. This property is at the root of the self-collimation effect [3–8], as the plane-wave components of the beam with wave vectors lying on the plateau do not dephase in the propagation and do not lead to the diffrac-

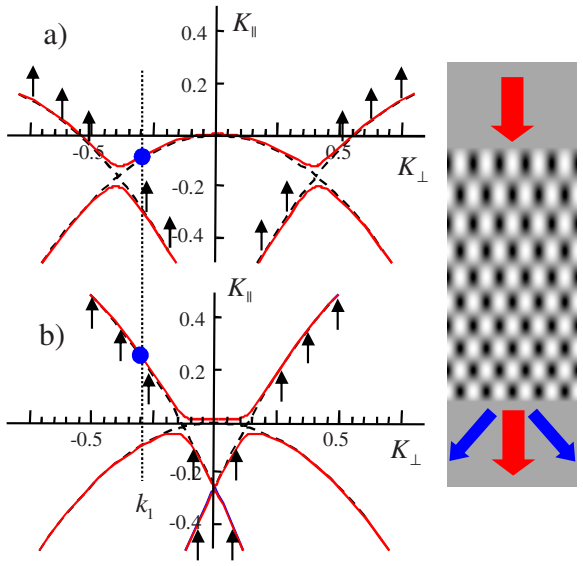

FIG. 2. (Color online) The dispersion curves in the PC with chirp: (a) at the entrance, where $Q_\parallel(0)=0.2$, (b) at the rear face, where $Q_\parallel(L)=0.75$, $f=0.04$. The circle indicates the particular harmonics transferred from one spatial oscillator to another (dashed curves), or equivalently, remaining on the same Bloch mode (solid lines). The arrows indicate the deformation of the dispersion curves along the chirped PC. The picture at the right illustrates the chirped PC.

tive spreading of the constituent beam. Most significant to our study is that the same dispersion curve also displays strongly pronounced slopes. The basic idea of the present paper is that these slopes could be used for spatial filtering, as the radiation lying on the slopes is strongly deflected in the propagation through the PC. The propagation is directed along the gradient of frequency $\vec{v}=d\omega/d\vec{K}$, therefore is perpendicular to the dispersion curve in the space $\vec{K}=(K_\perp,K_\parallel)$, as illustrated the by thick arrows in Fig. 1.

IV. CHIRPED CASE

The problem is, however, that the incoming radiation projects very weakly onto the segments of the "tilted" Bloch modes (indicated by *b* in Fig. 1) because in these segments the plane-wave components are almost orthogonal to the corresponding Bloch modes. The efficiency of the projection into the Bloch modes is inversely proportional to the distance between the dispersion curves of the Bloch modes (solid lines) and the dispersion curves of corresponding plane waves (dashed lines) [9]. Therefore the radiation projects essentially onto the *a* and the *c* segments of the Bloch modes, and the expected filtering function, which is related with the tilted *b* segments, is inactive. The projection problem can be overcome by using the longitudinally chirped PC. The idea is illustrated in the Fig. 2. The longitudinal period at the entrance of the PC is chosen as corresponding to Fig. 2(a), in order to project efficiently all the radiation from the entire spatial spectrum of the beam onto the basic Bloch mode. Along the PC the period decreases [$Q_\parallel(Z)$ increases] and the dispersion diagram deforms continuously (illustrated by the arrows in Fig. 2). At the rear face of the PC, the period is such that the spatial dispersion curve attains the shape shown in Fig. 2(b). If the chirp is sufficiently weak, the process can be considered as adiabatic. Then, the occupations of the Bloch modes remain unchanged and all the excitation is projected to the strongly tilted segments of the Bloch mode (segments *b*) and eventually deflected.

V. NUMERICAL PROOF

We prove the above-described idea by the numerical simulation of the paraxial model (1) in two dimensional (2D) demonstrating the predicted effect of spatial filtering. We consider the harmonic modulation of the index with the PC and assume that the beam enters from and leaves to the region with the same refraction index as in the PC, but with no index modulation. The results are presented in Fig. 3. In Figs. 3(a) and 3(b) the input is a narrow beam, with sufficiently broad spatial spectrum (broader than the width of the plateau at the rear face of the PC). When the PC is without chirp, the filtering is absent, and only narrow areas from the central maximum of the spatial spectrum of the beam are deflected [Fig. 3(a)]. The dips occur at the cross points of the dispersion curves of the harmonic components due to two reasons: the projection of the plane waves into the Bloch modes at the entrance of the PC (the plane waves project equally on both Bloch modes at the cross point of the dispersion curves of the harmonic components) and the back projection of the excitation of the Bloch modes into the plane waves at the rear face of the PC. The latter projection depends on the length of the PC, i.e., depends on with which phase difference the both Bloch modes arrive to the rear face of the PC. In average, half of the radiation remains in the central maximum and half goes to the first maxima at the angles corresponding to the cross points of the plane-wave components. In case of the chirped PC [Fig. 3(b)] the radiation projects efficiently onto the slopes, as described above, and during the propagation through the PC is transported to the sidebands and deflected with almost 100% efficiency.

As the effect is linear then the different spatial components of the radiation can be treated separately; thus the filtering process illustrated above with the regular beams works equally well with the noisy beams. Figure 3(c) shows the propagation of the beam with spatial phase noise, of approximately the same spatial spectrum width as in Figs. 3(a) and 3(b). As expected, the filtering works, resulting in an efficient cleaning of the beam.

VI. ESTIMATION OF THE MINIMUM LENGTH OF PC

The ideal filtering can be realized in the adiabatic limit, when the chirp is very weak, and, respectively, when the PC is extremely long. In practice, however, this limit is difficult to realize. It is significant, therefore, to evaluate the minimum length of the PC that can ensure the reasonable filtering. The process of projection of the radiation onto the slopes is described by Eq. (3). By fixing a particular transverse wave number $K_\perp$ (indicated in Fig. 2 by a vertical dotted line), one can restrict the analysis to that of two coupled

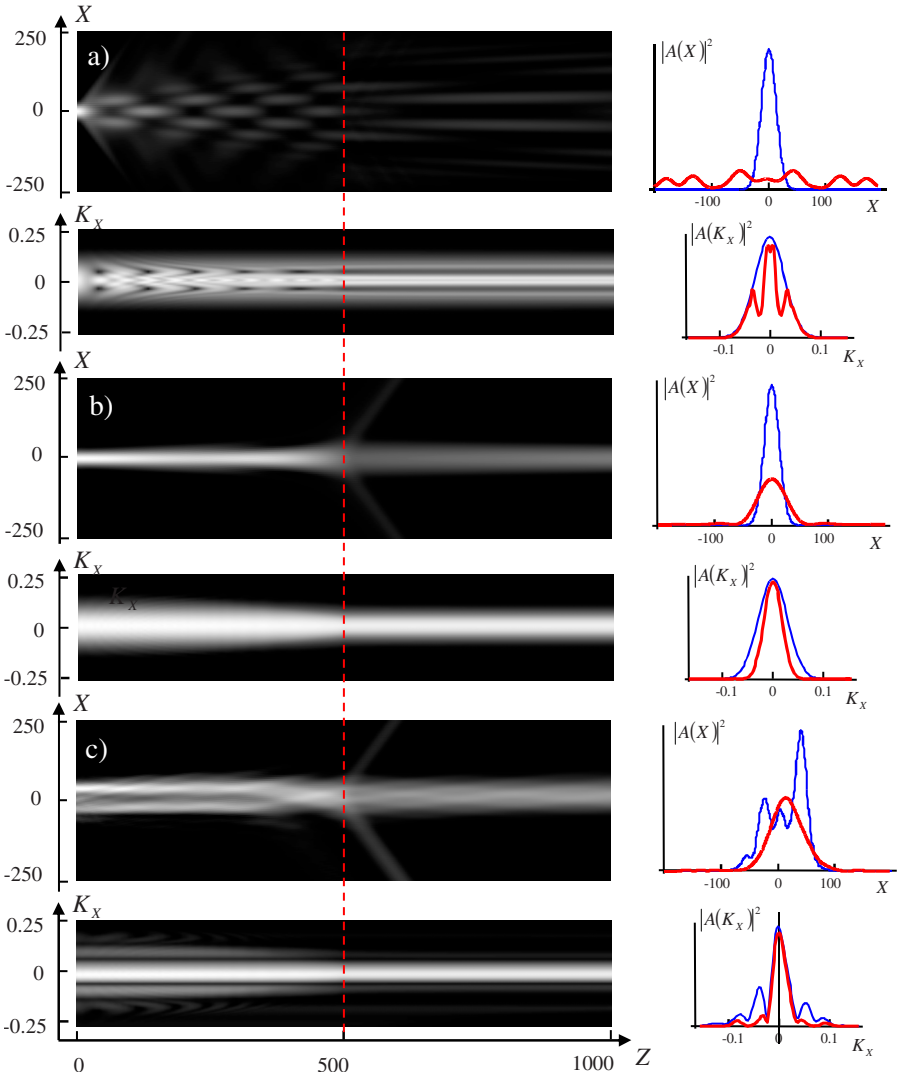

FIG. 3. (Color online) Propagation of the beams through the PCs. (a) Regular beam propagating through the unchirped PC with $Q_{\|}(0)=Q_{\|}(L)=0.92$ and (b) through the chirped PC with $Q_{\|}(0)=0.61$, $Q_{\|}(L)=0.92$; (c) noisy beam, with the width of the spatial spectrum approximately equal to that in cases (a) and (b) propagating through the chirped crystal as in (b). In all cases $f=0.022$. On the right-hand side, the field distributions are shown [at the entrance of the crystal at $Z=0$ (thin, blue line) and well behind the crystal at $Z=1000$ (thick, red line)] both in space- and spatial-spectra domain. The dashed line indicates the rear face of the crystal (at $Z=500$). The normalized chirp parameter is $\beta=\alpha/f^2=1.24$ in cases (b) and (c).

spatial oscillators (two harmonics) participating in the excitation exchange process. The other harmonics, being far from resonance, does not interfere the process under the study. From Eqs. (3) we obtain

$$\frac{dA_1(Z)}{dZ} = ifA_2(Z), \tag{4a}$$

$$\frac{dA_2(Z)}{dZ} = i\Delta Q_{\|}(Z)A_2(Z) + ifA_1(Z), \tag{4b}$$

where $(A_1,A_2)=(A_{0,0},A_{-1,-1})e^{iK_{\perp}^2 Z}$. The reference propagation wave number is fixed to that of the zero harmonics, and $\Delta Q_{\|}(Z)=Q_{\|}(Z)-(K_{\perp}-1)^2+K_{\perp}^2$ is the mismatch between the propagation wave numbers of both considered spatial harmonics.

The scenario of energy exchange is as follows: initially the first oscillator is excited [i.e., the one belonging to the harmonics $\vec{Q}_{0,0}=(0,0)$]. Along the crystal the spatial frequency of the second oscillator [belonging to $\vec{Q}_{-1,\pm 1}=(-1,\pm Q_{\|})$] is varied, as illustrated in Fig. 4(a). We expect that at the end of the procedure, the radiation transfers to the second oscillator, equivalently, the excitation remains on the same Bloch mode. Figure 4(b) shows the evolution of the excitation of the oscillators for the linear chirp $\Delta Q_{\|}(Z)=\alpha Z$. In the weak chirp case ($\alpha \ll f^2$), the excitation indeed remains on the same Bloch mode (equivalently, transfers from one spatial harmonics to the other). The transfer occurs essentially in the (longitudinal) segment of the PC corresponding to the resonance between the interacting spatial harmonics, i.e., when $|\Delta Q_{\|}(Z)| \leq f$. In the case of the strong chirp, the situation is opposite: the radiation is exchanged between the both Bloch modes and equivalently remains on the same spatial harmonics. The latter situation is related with the Landau-Zener-type tunneling between two Bloch modes during the fast (nonadiabatic) processes [10].

The parameters of Eq. (4) can be scaled, leading to only one free parameter: the normalized strength of the linear chirp $\beta=\alpha/f^2$. This implies that the excitation transfer (and eventually the efficiency of filtering) depends solely on that parameter β. A numerical study of the efficiency of the excitation transfer based on Eq. (4) shows that, e.g., a projection of 50% of the excitation to the slopes occurs at $\beta_{50\%} \approx 9 \pm 0.2$, a projection of 90% occurs at

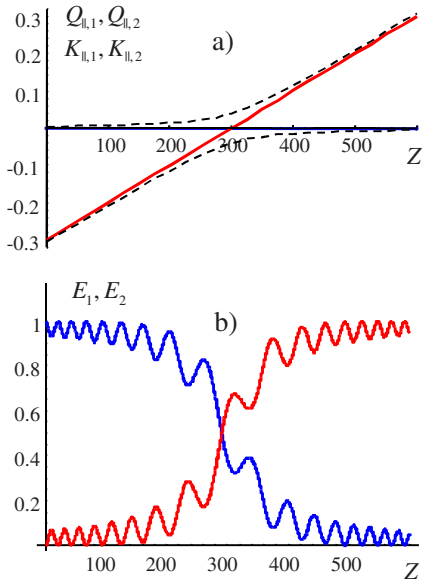

FIG. 4. (Color online) (a) The longitudinal propagation wave numbers of the harmonic components (solid lines) and the wave numbers of the Bloch modes (dashed lines) along the chirped PC. (b) Variation in the excitation of the two harmonic components. Parameters $\alpha=0.001$, $f=0.04$ (the normalized chirp is $\beta=\alpha/f^2=0.625$).

$\beta_{90\%}\approx 2.7\pm 0.05$, and a projection of 99% occurs at $\beta_{99\%}\approx 1.25\pm 0.02$ [11].

VII. REAL WORLD PARAMETERS

We estimate the physical parameters required for the efficient filtering. In order to make the effect of filtering useful (to filter out the substantial part of the spatial spectrum of the beam) the condition $|\Delta Q_{\|}|\approx 1$ is to be fulfilled, which means that the cross point of dispersion curves moves over nearly all the spatial spectra. Assuming the limit $f\ll 1$, this leads to the estimation for the PC length (in terms of longitudinal periods of the PC N) $N\geq(2\pi\beta f^2)^{-1}$, or in terms of original variables $N\geq 2(q_\perp/k_0)^4/(\pi\beta\Delta n^2)$. We estimated the PC filter thickness for several cases: (i) for conventional glasses with weakly modulated index [$\Delta n\approx 10^{-4}$ and $(k_0/q_\perp)\approx 10$] (fabricated, e.g., by laser-pulse writing technique [12]), the 90% filtering requires $N\geq 2000$ longitudinal periods. (ii) For special glasses of photorefractive crystals with moderately modulated index [$\Delta n\approx 10^{-3}$ and $(k_0/q_\perp)\approx 10$] (see, e.g., [13] for glasses, and [14] for photorefractive crystals) the 90% filtering should be observable for the PCs as long as containing $N\geq 20$ longitudinal periods. (iii) For high contrast PCs [$\Delta n\approx 0.1-1$ and $(k_0/q_\perp)\approx 1$] (see, e.g., [12]), the above estimation states that the filtering is efficient for the length of the crystal of order of one period, i.e., does not impose any minimum length of the PC. The latter result gives a hope that the efficient filtering could be achieved in very short PCs, just containing several longitudinal periods. This case is however to be studied separately, most likely solving the full Maxwell equations (e.g., using the finite difference time domain techniques) as the paraxial approximation (1) is no more valid in this case [15].

The above estimations refer to the "utile" filtering, which means that the large part of the spatial spectrum is deflected with nearly the 100% efficiency. For the experimental proof of the effect (just in order to make the effect of the chirp visible, i.e., to distinguish from the unchirped case), one needs to fulfill the weaker condition $|\Delta Q_{\|}|\geq f$, i.e., one needs to sweep the longitudinal propagation wave vector so that the cross point of the spatial dispersion curves more than over the width of the dip in the unchirped case. The estimation of the number of the longitudinal periods of the PC necessary for the observation of filtering $N\geq(2\pi\beta f)^{-1}$, or in terms of original variables $N\geq(q_\perp/k_0)^2(\pi\beta\Delta n)^{-1}$, which results in significantly shorter crystals than estimated above for reasonable filtering. In particular, the effect of filtering in weakly modulated index case [$\Delta n\approx 10^{-4}$ and $(k_0/q_\perp)\approx 10$] should be visible for the PC as short as $N\geq 10$ longitudinal periods.

VIII. CONCLUSIONS

We predict and show the possibility of spatial filtering in longitudinally chirped PCs. We evaluated the parameters of the PC, concluding that they are reasonable for the experimental demonstration, as well as for the technological implementation of the effect. The filtering effect can be shown for the PCs with high and the low modulations of refraction index; for the reasonable filtering of the light beam the index modulation of $\Delta n\approx 10^{-2}$ seems to be optimal. The filtering has been demonstrated numerically in the case of harmonic modulation of the refraction index, but the idea is also applicable also to "usual" PCs, where due to the microfabrication techniques the refraction index profile is sharp.

The presented analysis concerns the 2D case, i.e., the beams with one transverse dimension propagating in 2D PC, but could be also extended into the 3D case. The mechanism of the projection on the slopes of the dispersion surfaces and the estimated values of the chirp remains the same as in 2D case. The essential difference with the 2D case is the symmetry of the lattice in the transverse plane of the [7]. It comes out from a preliminary study that the different symmetries of the PC in transverse plane result in the different shape of the spot in the spatial Fourier domain, e.g., a square lattice results in a square filter pass window. Reasonable filters for applications should be of hexagonal or of octagonal symmetry.

The method can be optimized. In order to achieve a larger projection into the Bloch modes not only the longitudinal period but also the other parameters could be varied. For example, as shown in [16], the slow variation in the index modulation amplitude (the hole radius) can improve the transfer of energy. Also a special function of the chirp can be used, instead of the linear one considered in the present work, which might optimize the properties of the filter. It also should be noted that the sign of the chirp could also be reversed.

We note that the effect of filtering is applicable for other sorts of waves. The filtering of sound waves follows straightforwardly from the above study due to the similarity of the wave description in these systems. The cleaning of the BECs

requires, however, a special geometry. As the propagation in optics corresponds to the time evolution in BECs then the 2D PC corresponds to the modulated in time and space potential of the BEC, as discussed in [6,7]. The longitudinal chirp in optics then corresponds to the smooth (adiabatic) variation in the temporal modulation frequency in the case of BECs.

ACKNOWLEDGMENTS

The work was financially supported by Spanish Ministerio de Educación y Ciencia and European Union FEDER through Projects No. FIS2005-07931-C03-02, and-03 and No. FIS 2008-06024-C02-02 and-03.

[1] A. E. Siegman, Proc. SPIE **1868**, 2 (1993).
[2] P. Hariharan, *Optical Holography* (Cambridge University Press, Cambridge, UK, 1996), pp. 74–75.
[3] H. Kosaka *et al.*, Appl. Phys. Lett. **74**, 1212 (1999).
[4] D. N. Chigrin *et al.*, Opt. Express **11**, 1203 (2003); R. Iliew *et al.*, Appl. Phys. Lett. **85**, 5854 (2004); D. W. Prather *et al.*, Opt. Lett. **29**, 50 (2004).
[5] K. Staliunas and R. Herrero, Phys. Rev. E **73**, 016601 (2006).
[6] K. Staliunas, R. Herrero, and G. J. de Valcárcel, Phys. Rev. E **73**, 065603(R) (2006).
[7] K. Staliunas, R. Herrero, and G. J. de Valcárcel, Phys. Rev. A **75**, 011604(R) (2007).
[8] I. Pérez-Arjona *et al.*, Phys. Rev. B **75**, 014304 (2007); V. Espinosa *et al.*, *ibid.* **76**, 140302(R) (2007).
[9] The efficiency of the projection is in general determined by the vector product between the eigenvectors of Bloch mode with the vector of the corresponding plane-wave component. The study of the projection in the particular case studied is to be published elsewhere.
[10] C. Zener, Proc. R. Soc. London, Ser. A **137**, 696 (1932).
[11] The detailed study of the excitation reprojection in Eq. (4) is to be presented elsewhere.
[12] K. Busch *et al.*, Phys. Rep. **444**, 101 (2007).
[13] O. M. Efimov, L. B. Glebov, and V. I. Smirnov, Opt. Lett. **25**, 1693 (2000).
[14] D. Neshev *et al.*, Phys. Rev. Lett. **93**, 083905 (2004).
[15] We note that the expansion (2) leading to Eq. (3) is possible without paraxial approximation, and the discussions concerning the projecting of the excitation on the slopes of dispersion curves is qualitatively correct also for nonparaxial case. In this nonparaxial case, the dispersion curves are circles instead of parabolas in the paraxial case considered in the present paper.
[16] B. Momeni and A. Adibi, Appl. Phys. Lett. **87**, 171104 (2005).